Proton conducting intermediate-temperature solid oxide fuel cells using new perovskite type cathodes

CrossMark

Meiling Li [a,b], Meng Ni [a,*], Feng Su [b], Changrong Xia [b,1]

[a] Department of Building and Real Estate, The Hong Kong Polytechnic University, Hong Kong, China
[b] Department of Material Science and Engineering, University of Science and Technology of China, Hefei, Anhui, China

HIGHLIGHTS

- $Sr_2Fe_{1.5}Mo_{0.5}O_{6-\delta}$ (SFM) is used as cathode for H-SOFC.
- SFM is compatible with BCZY electrolyte under 1100 °C.
- SFM—BCZY cathode is promising for H-SOFC at intermediate temperature.
- Good performance is achieved with SFM—BCZY composite cathode.
- Co-sintering temperature of 1000 °C is found optimal.

ARTICLE INFO

ABSTRACT

$Sr_2Fe_{1.5}Mo_{0.5}O_{6-\delta}$ (SFM) is proposed as the electrodes for symmetric solid oxide fuel cells (SOFCs) based on oxygen-ion conducting electrolytes. In this work SFM is investigated as the cathodes for SOFCs with proton conducting $BaZr_{0.1}Ce_{0.7}Y_{0.2}O_{3-\delta}$ (BZCY) electrolyte. SFM is synthesized with a combined glycine and citric acid method and shows very good chemical compatibility with BZCY under 1100 °C. Anode-supported single cell (Ni—BZCY anode, BZCY electrolyte, and SFM-BZCY cathode) and symmetrical fuel cell (SFM—BZCY electrodes and BZCY electrolyte) are fabricated and their performances are measured. Impedance spectroscopy on symmetrical cell consisting of BZCY electrolyte and SFM—BZCY electrodes demonstrates low area-specific interfacial polarization resistance R_p, and the lowest R_p, 0.088 Ω cm^2 is achieved at 800 °C when cathode is sintered at 900 °C for 2 h. The single fuel cell achieves 396 mW cm^{-2} at 800 °C in wet H_2 (3 vol% H_2O) at a co-sintering temperature of 1000 °C. This study demonstrates the potential of SFM—BZCY as a cathode material in proton-conducting intermediate-temperature solid oxide fuel cells.

1. Introduction

Solid Oxide Fuel Cell (SOFC) is a high temperature (600—1000 °C) power generator, which can convert the chemical energy of a fuel to electrical energy directly via electrochemical reactions [1,2]. The energy efficiency of SOFC is not limited by Carnot efficiency and is considerably higher than conventional heat engines. The high operating temperature enables direct internal reforming of hydrocarbon fuels or thermal decomposition of ammonia in the porous anode of SOFC, thus SOFC is capable of using various alternative fuels, including hydrogen, methane, natural gas, ammonia, and renewable biogas. Moreover, the waste heat from SOFC stack is of high quality and can be recovered by integrating SOFC with other systems for combined thermal (heating or cooling) and power co-generation, leading to high system efficiency. Due to these advantages, SOFC has received significant attention as a promising alternative power sources for a variety of applications with various fuels [3]. According to the type of electrolyte materials used, SOFC can be divided into two main types: proton conducting solid oxide fuel cell (H-SOFC) and oxygen ion conducting solid oxide fuel cell (O-SOFC).

Key issues that hinder the widespread application of SOFC include high cost and long-term performance degradation. It has been observed that performance degradation of SOFC is usually caused by coarsening of the catalyst particles, sulfur poisoning, or carbon deposition. In recent years, novel symmetrical fuel cell (SFC) has been proposed [4—6]. In an SFC, the use of same ceramic material as both the anode and cathode not only simplifies the

* Corresponding author. Tel.: +852 27664152; fax: +852 27645131.
E-mail addresses: bsmengni@polyu.edu.hk, memni@graduate.hku.hk (M. Ni), xiacr@ustc.edu.cn (C. Xia).
[1] Tel.: +86 0551 63607475; fax: +86 0551 63601592.

fabrication process, but also solves the carbon deposition problem as the deposited solid carbon can be removed simply by shifting the anode and cathode [7].

In addition, the high cost and catalyst coarsening can be solved by lowering the operating temperature of SOFC to an intermediate temperature (IT) range as low-cost materials can be used in SOFC and the sintering of porous electrodes at IT is greatly slowed down [8]. The performance of SOFC at reduced temperature with conventional materials is also low due to low ionic conductivity of the yttria-stabilized zirconia (YSZ) and high polarization loss of the LSM-based cathode. To improve the SOFC performance at IT, alternative electrolyte materials with good ionic conductivity and cathode materials with good catalytic activity towards oxygen reduction reaction (ORR) have been developed. BZCY is a potential electrolyte material for practical IT-SOFCs due to its good proton conductivity at a reduced temperature and good chemical compatibility with other SOFC components. In addition to its good proton conductivity, the use of proton conductor as electrolyte also leads to a higher Nernst potential (thus a higher maximum efficiency) since H_2O is produced in the cathode, which in turn increases the molar fraction of H_2 in the anode. With NiO–BZCY|BZCY|$Sm_{0.5}Sr_{0.5}Co_{3-\delta}$ (SSC)–BZCY configuration, an anode supported SOFC achieved a peak power density of 650 mW cm^{-2} at 700 °C [9] (detailed output performance data of SOFCs with different configurations or materials are listed in Table 1). In advanced H-SOFC with thin film electrolyte (about 10 μm), the polarization loss of the cathode could account for up to 50% of the total over-potential loss. To further improve the cell performance, new cathode materials have been developed by many researchers for H-SOFCs based on BZCY electrolyte, such as $La_{0.7}Sr_{0.3}FeO_{3-\delta}$–$Ce_{0.8}Sm_{0.2}O_{2-\delta}$ (LSF–SDC) [10], $Sm_{0.5}Sr_{0.5}Co_{3-\delta}$–$Ce_{0.8}Sm_{0.2}O_{2-\delta}$ (SSC–SDC) [11], $Ba_{0.6}Sr_{0.4}Co_{0.9}Nb_{0.1}O_3$ (BSCN) [12], $GdBaCo_2O_{5+\delta}$ [13], and good performances have been obtained.

Due to the diverse conduction mechanisms, cathode materials of H-SOFCs can be classified into 3 main types [14]: (1) electronic conductor single phase cathode (i.e. Pt); (2) mixed electronic and oxygen ion conducting single phase (i.e. $La_{0.7}Sr_{0.3}MO_3$ [15], $Ba_{0.5}Sr_{0.5}Co_{0.8}Fe_{0.2}O_3$ (BSCF) [16]) or composite cathodes (i.e. $Sm_{0.5}Sr_{0.5}Co_{3-\delta}$–$Ce_{0.8}Sm_{0.2}O_{2-\delta}$ (SSC–SDC) [11], and $Sm_{0.5}Sr_{0.5}Fe_{0.8}Cu_{0.2}O_3$–SDC [17]); and (3) mixed electronic and proton conducting single phase (i.e. $BaCe_{0.5}Bi_{0.5}O_3$ [18] and $BaCe_{0.5}Fe_{0.5}O_3$ [18]) or composite cathodes (i.e. SSC-$BaCe_{0.5}Sm_{0.2}O_3$ (BCS) [20]). Many perovskite materials containing transition metal ions are known to be mixed ionic–electronic conductors (MIEC), which can be applied as both cathode and anode materials in IT-SOFCs, such as Sr-doped $LaFeO_3$ (LSF), Sr-doped $LaCoO_3$ (LSC), Sr-doped La (Co, Fe)O_3 (LSCF) [21]. The perovskite $Sr_2Fe_{1.5}Mo_{0.5}O_6$ (SFM) shows high redox stability and has been studied by many research groups for its possible use as SOFC electrodes. Due to its mixed Fe^{3+}/Fe^{2+} and Mo^{6+}/Mo^{5+} valences, SFM is proved to be a MIEC material [22]. Single fuel cells with the configuration of SFM|$La_{0.8}Sr_{0.2}Ga_{0.83}Mg_{0.17}O_3$ (LSGM)| $Ba_{0.5}Sr_{0.5}Co_{0.8}Fe_{0.2}O_3$ (BSCF) exhibits a remarkable electrochemical activity in H_2 and achieves a peak power density of 603 mW cm^{-2} at 800 °C [23]. Remarkable cell performances are also achieved using SFM and other material (i.e. SFM–SDC [24,25]) as composite cathodes for IT-SOFCs in humidified H_2. Compared with single phase SFM electrode fuel cells, nano-structured SFM electrode by infiltrating $Ce_{0.8}Sm_{0.2}O_{1.9}$ (SDC) nanoparticles onto the SFM backbone greatly decreases the interfacial polarization resistance of SDC electrolyte symmetrical fuel cells from 0.27 Ω cm^2 to 0.11 Ω cm^2 at 750 °C [26].

Despite of their potential for electrolyte and cathode materials in O-SOFC, the feasibility of BZCY–SFM composite cathode in H-SOFC has not been evaluated yet. To fill the research gap, this study is purposely designed to evaluate the feasibility of SFM as a cathode

Table 1
Output performance of fuel cells with different configurations (different cathode materials).

Fuel cells of different configuration with different cathode materials	Interfacial polarization resistance R_p (Ω cm²)	Operating temperature t_{op} (°C)	Peak power density (mW cm⁻²)
NiO–BZCY|BZCY|SSC–BZCY [9]	NA	700	650
SFM|LSGM|BSCF [23]	NA	800	603
SFM infiltrated with nano-SDC| SDC [26]	0.27–0.11	750	NA
SFM|LSGM|SFM [32]	0.26	900	NA
LSCT|LSGM [5]	NA	800	220
BSCF–SFM|BZCY|NiO–BZCY [35]	0.46	600	NA
BCFN|BZCY|NiO–BZCY [12]	0.10	700	NA
BCBN|BZCY [18]	0.28	700	NA
$Pr_2NiO_4+\delta$|BZCY [36]	2.76	600	NA
$Sm_{0.5}Sr_{0.5}FeO_{3-\delta}$–BZCY|BZCY [33]	0.10	700	341
SSC–BCS as cathode [20]	0.21	700	NA
$GdBaCo_2O_5+\delta$|BZCY [13]	0.16	700	NA
$SmBaCo_0O_5+\delta$|BZCY [37]	0.15	700	NA
$PrBaCo_2O_5+\delta$|BZCY [38]	0.15	700	NA
LSF–SDC|BZCY [10]	0.074	650	542

material for H-SOFCs. Anode-supported H-SOFCs are fabricated with the perovskite-type $Sr_2Fe_{1.5}Mo_{0.5}O_6$–$BaZr_{0.1}Ce_{0.7}Y_{0.2}O_{3-\delta}$ (SFM–BZCY) composite cathode, BZCY electrolyte, and NiO–BZCY anode. Symmetrical fuel cells are also made with SFM–BZCY as both electrodes. Both the single fuel cells and symmetrical fuel cells are characterized and tested. In addition, the effects of sintering temperature on the microstructure and cell performance are investigated.

2. Experimental

2.1. Material preparation and powder synthesis

$Sr_2Fe_{1.5}Mo_{0.5}O_6$ (SFM) was synthesized by a microwave-assisted combustion method using $Sr(NO_3)_2$ (AR), $Fe(NO_3)_3 \cdot 9H_2O$ (AR) and $(NH_4)Mo_7O_{24} \cdot 4H_2O$ (AR, Sinopharm Chemical Reagent Co., ltd) as the starting metal materials. Glycine and citric acid were used to assist the combustion process. And the mixing process was conducted with continuous stirring and heating for 1 h to form first-step aqueous solution, which was subsequently heated to self-combustion, resulting in black ash. Then, the as-prepared ash was calcined at 1000 °C for 5 h to form dark SFM powders with perovskite structures, which were confirmed with X-ray diffraction (XRD) measurement.

The BZCY electrolyte powders were synthesized through a citric acid–EDTA sol–gel process. Y_2O_3 was dissolved in concentrated nitric acid, and the stoichiometric amounts of $Zr(NO_3)_4 \cdot 5H_2O$, $C_4H_6BaO_4$, $(NH_4)_2Ce(NO_3)_6$, and $Ce(NO_3)_3 \cdot 6H_2O$ (all in 99.9%, Sinopharm Chemical Reagent Co., ltd) were added into the aqueous solution sequentially with continuously stirring for 2 h. Then concentrated ammonia was applied to adjust the solution pH to ~6.0. A final viscous gel would be obtained after continuously heating and stirring, which would be pre-heated at about 300 °C for 3~4 h to get white ash-like material and be further calcined at 1000 °C in air for 5 h to obtain a BZCY perovskite.

2.2. Characterization

To investigate their chemical compatibility, SFM and BZCY were mixed, uniaxially pressed into pellets, and heated at 900 °C, 1000 °C and 1100 °C for 2 h. The phase structures of the heated pellets were analyzed using XRD (Riguku-TTR III) with Cu-Kα radiation under the scanning rate of 10 °C min^{-1}. The cross-section and detailed morphology of the single cell after electrochemical tests was
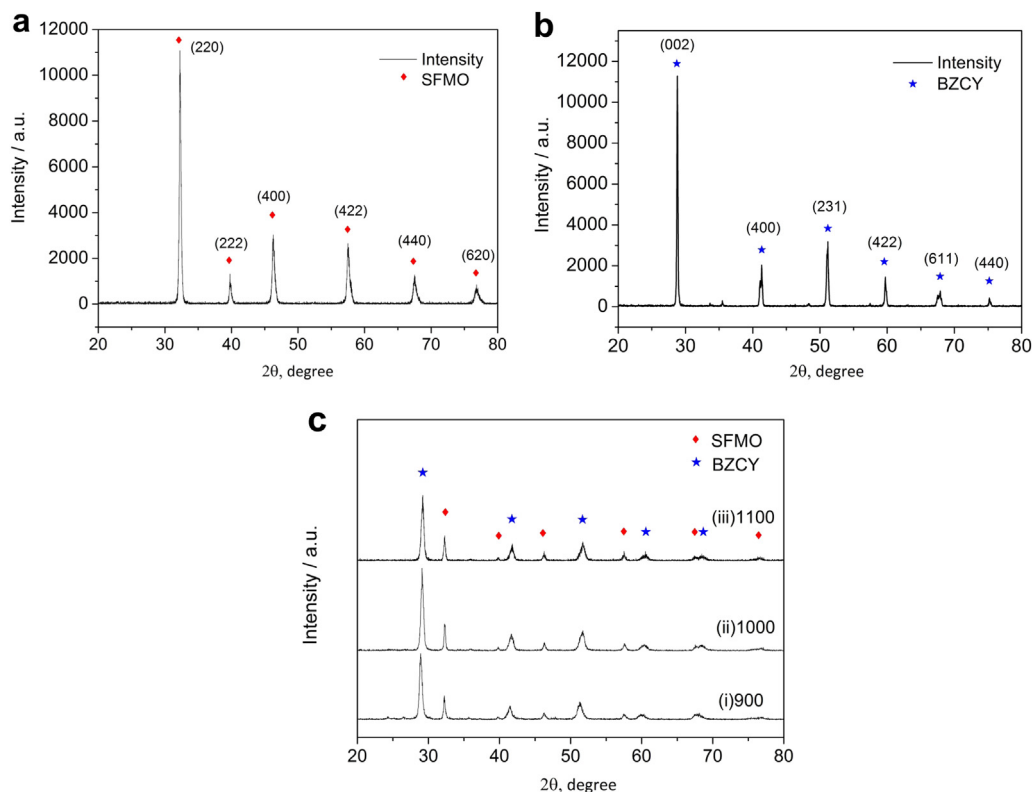
Fig. 1. XRD patterns of (a) $Sr_2Fe_{1.5}Mo_{0.5}O_{6-\delta}$ (SFM) powder; (b) $BaZr_{0.1}Ce_{0.7}Y_{0.2}O_{3-\delta}$ (BZCY) powder; (c) mixed powders of SFM−BZCY (40:60 weight%) fired at (i) 900 °C for 2 h in air atmosphere (ii) 1000 °C for 2 h in air atmosphere (iii) 1100 °C for 2 h in air atmosphere.

characterized by JEOL JSM-6700F scanning electron microscope (SEM) instrument. All electrochemical characteristics of single fuel cells and symmetrical fuel cells were tested by AC impedance spectra method inserted in a synchronous electrochemical workstation (Solartron, No. 1260A and 1287A). The applied frequency ranged from 0.01 Hz to 1000 kHz with a signal amplitude of 30 mV under open-circuit conditions.

2.3. Cell fabrication and test settings

Anode supported single fuel cells were pressed into slice by two steps that loose BZCY electrolyte powder was co-pressed under 8 MPa pressure to previously formed thick anode. And all composite SFM−BZCY cathode starches were thinly printed to the BZCY electrolyte.
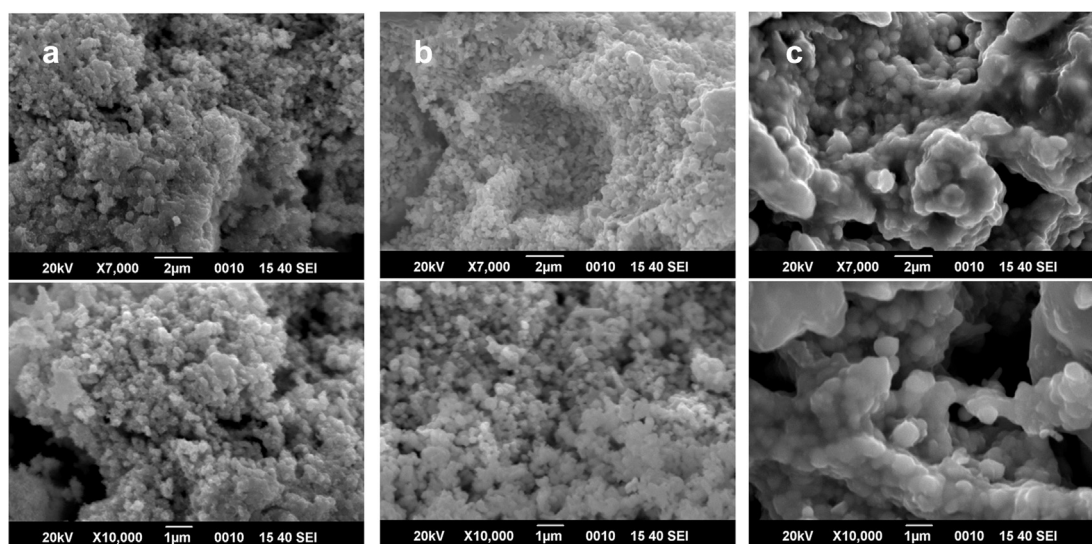

Fig. 2. Micrograph SEM images of SFM−BZCY composite cathodes co-sintered at (a) 900 °C; (b) 1000 °C; (c)1100 °C; (×7000 and 10,000 times, respectively) of symmetrical fuel cells (SFCs).
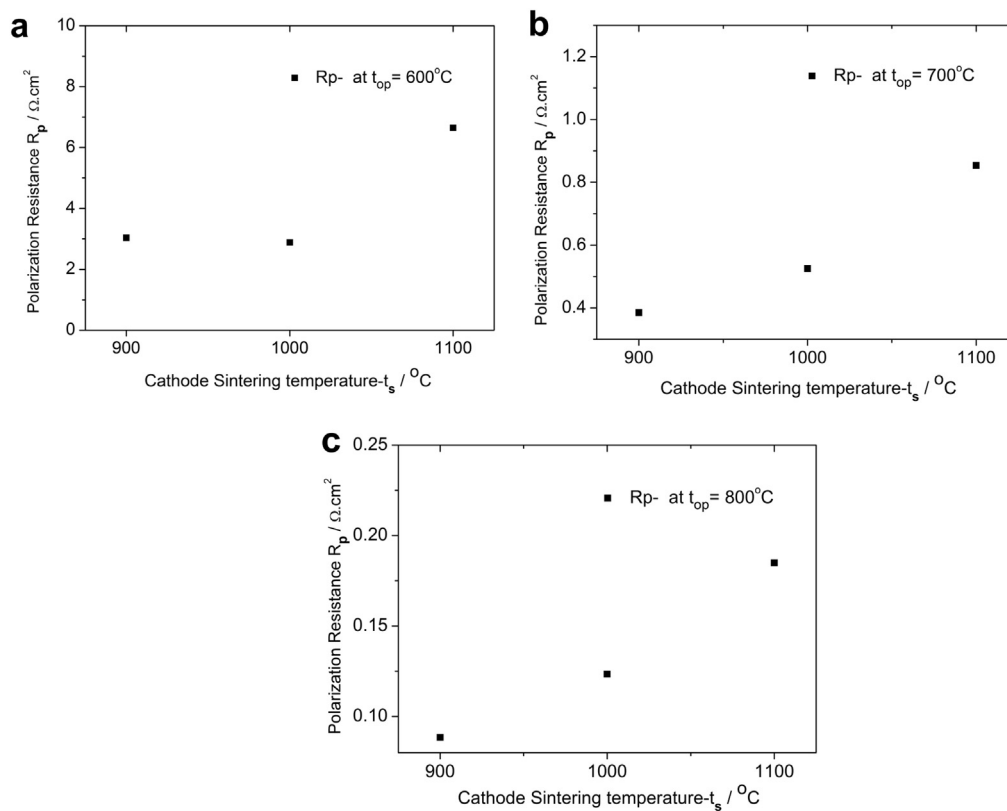
Fig. 3. Relationships between polarization resistance and cathode sintering temperature at certain operating temperature of: (a) 600 °C; (b) 700 °C; (c) 800 °C.
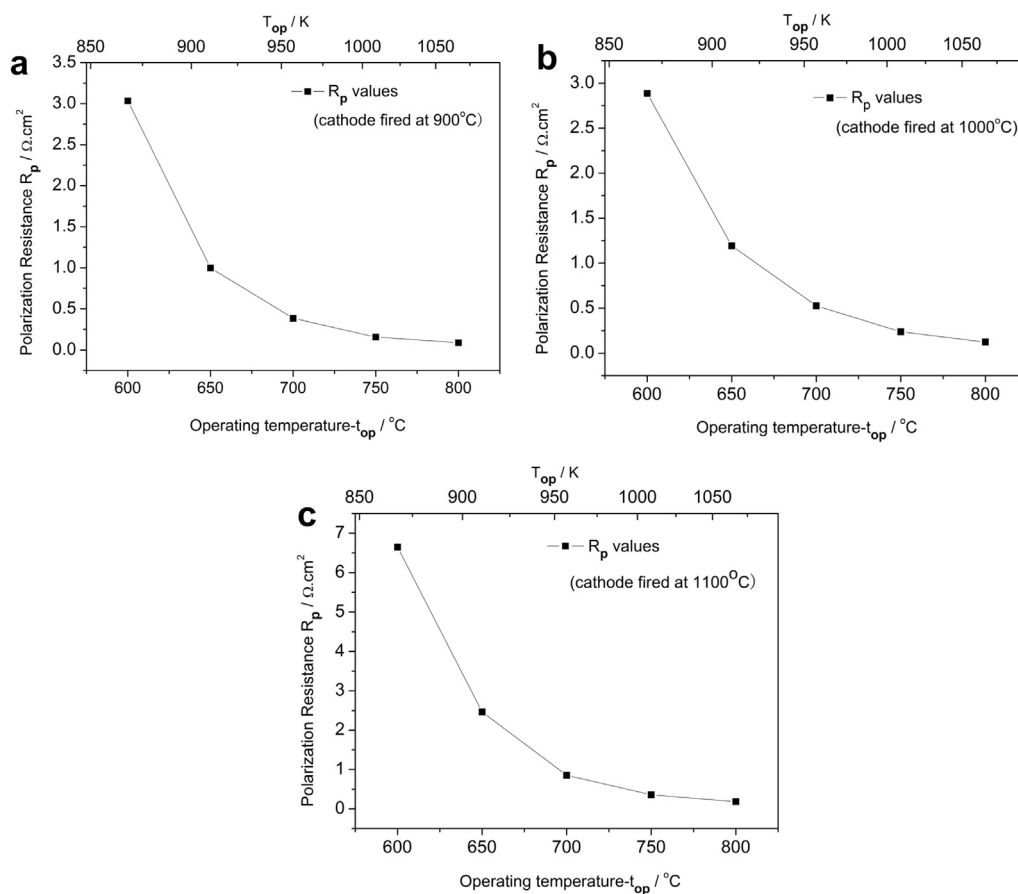

Fig. 4. Polarization resistance changing trends with different operating temperatures SFM−BZCY|BZCY|SFM−BZCY symmetrical fuel cells by cathode fired at: (a) 900 °C; (b) 1000 °C; (c)1100 °C.

2.3.1. Single fuel cell

The anode supported single fuel cells with the configuration of NiO−BZCY|BZCY|SFM−BZCY were tested in the temperature range of 600 °C−800 °C under normal atmospheric pressure. The single fuel cell slice was adhesive to a vertical special test tube by Ag paste used as current collection helper, and wet H_2 (3% H_2O) was fed into the anode side as fuel gas while cathode was exposed to ambient air oxidant. Cathodes of single fuel cells in this work were co-sintered under three different situations of 900 °C, 1000 °C and 1100 °C. The cell voltage was reduced from open circuit voltage (OCV) by a step of 30 mV and a maintenance period of 20 s for each step to get a stable performance during all the fuel cell electrochemical measurements.

2.3.2. Symmetrical fuel cell

Electrolyte supported symmetrical fuel cells (SFCs) with the configuration of SFM−BZCY|BZCY|SFM−BZCY were evaluated by horizontal electrochemical test tube equipments by connecting to the electrochemical workstation. As well as situations of single fuel cells, SFCs also were set under three cathode sintering conditions. The electrolyte substrates were prepared by uni-axial pressing the BZCY powder at 200 MPa with a manual sheeter (KEQI 769YP-24B) and subsequently sintering at 1500 °C for 5 h in air. The sintered BZCY pellets had a diameter of 12.2 mm, a thickness of 0.55 mm. To fabricate the electrodes, SFM and BZCY powders were mixed at a mass ratio of 4:6 (a volume ratio of about 1:1) to prepare the print-ink with ethocel and abietyl alcohol as the organic binders. The inks were symmetrically printed onto each side of the BZCY substrate surface three times, dried and heated at three different sintering temperatures like 900, 1000, and 1100 °C for 3 h in air, resulting in porous SFM−BZCY electrodes on dense BZCY electrolyte with about 1.165 cm^2 effective electrode area. 15% amount of total electrode powders (SFM + BZCY) corn starch was added in for pores generation.

3. Results and discussion

3.1. Chemical compatibility between SFM and BZCY

The chemical and thermal compatibility between the mixed ionic and electronic conducting oxides and ionic conductor at operating temperature range should be taken into account at first, since it has significant effects on composite cathodes performance. As can be seen from Fig. 1a and b, XRD characterization presents that peak intensity values of SFM [23,24,27,28] and BZCY [29,30] powders exhibit good agreements with classical results. All three samples (SFM and BZCY composite cathode) are single-phase double perovskites with same intensity at specific angle as shown in Fig. 1c(i−iii). May be Mo element of SFM would have little evaporation or diffusion in the powder synthesis or cell fabrication process, but no obviously strange peak intensity is found in XRD results. Thus, no reflections of interfacial and solid phase reactions between two materials are detected. It indicates the great desirable chemical and thermal compatibility between SFMO and BZCY sintered at 900 °C−100 °C. According to a previous study, 1150 °C is an optimal sintering temperature for both pure SFM and SFM-SDC composite electrodes, as the lowest polarization resistance decreases with increasing sintering temperature not higher than 1150 °C [31]. This result demonstrates that 1100 °C should be the peak sintering temperature for SFM to stay a single-phase double perovskite structure.

3.2. Symmetrical fuel cells performance

3.2.1. Sintering temperature impacts on microstructure

SEM graphs of the SFM−BZCY composite powder after electrochemical tests. As expected, the grain size of SFM−BZCY composite
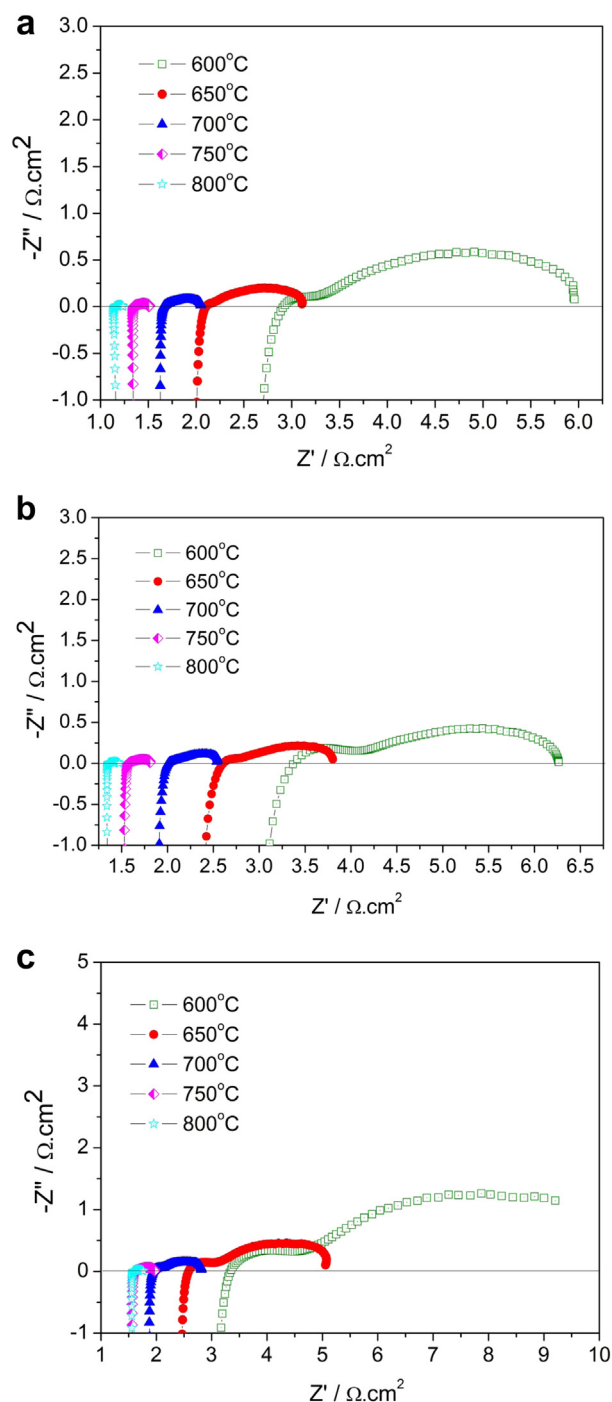
Fig. 5. Impedance spectra for symmetrical fuel cells with SFM−BZCY composite cathode measured at 5 different temperatures in range of 600 °C−800 °C (in steps of 50 °C) with various cathode sintering temperatures of (a) 900 °C; (b)1000 °C; (c) 1100 °C; in humidified air atmospheres (3% H_2O).

cathodes increases with the increasing sintering temperature as shown in Fig. 2. Meanwhile, the composite cathode phase has a relatively uniform size distribution with the average particle size ranging from 0.2 to 0.3 μm (fired at 900 °C), 0.3−0.5 μm (1000 °C), and 1−2 μm (1100 °C), respectively, which can demonstrate that cathode sintering temperature growth has promoting impacts on the microstructure of SFM−BZCY composite cathode by enlarging its grain size. Meanwhile, such obvious and typical porous
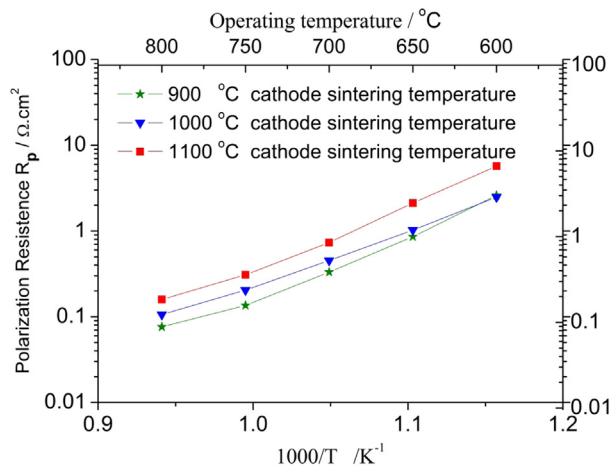
Fig. 6. Arrhenius plots of polarization resistance R_p of SFM–BZCY composite electrodes sintered at temperatures from 900 to 1000 °C.

electrode microstructure can provide more gas diffusion path and absorption site to exhibit high fuel cell performance.

3.2.2. Electrochemical performance of SFM–BZCY|BZCY symmetrical fuel cells

The electrochemical impedance spectra of symmetrical fuel cells with the configuration of SFM–BZCY|BZCY|SFM–BZCY are measured at operating temperature of 600–800 °C, and the results are analyzed in Figs. 3–5. The relationship between cathode sintering temperature t_s and polarization resistance R_p can be clearly found in Fig. 3, and lowest minimum R_p of 0.0884 Ω cm^2, 0.1234 Ω cm^2, and 0.1849 Ω cm^2 are achieved at 800 °C of SFC cathode fired at 900 °C, 1000 °C, and 1100 °C, respectively, which are even much better than R_p performance of 0.26 Ω cm^2 got by SFM|La$_{0.9}$Sr$_{0.1}$Ga$_{0.8}$Mg$_{0.2}$O$_3$ (LSGM)|SFM symmetrical fuel cell at 900 °C [32]. In general, for certain operating temperature, SFM–BZCY|BZCY SFCs show better performance with low R_p by cathode fired at 900–1000 °C. Meanwhile, the lowest values of R_{ohmic} are obtained as 1.1484 Ω cm^2, 1.3525 Ω cm^2, and 1.5838 Ω cm^2 at 800 °C. Therefore, the low R_p and R_{ohmic} demonstrate the good potential of SFM–BZCY as both an anode and cathode materials for H-SOFC at reduced temperature. It is clearly seen that the interfacial polarization resistance R_p decreases with increasing operating temperature for the three cathode firing cases in Fig. 4. Both the ohmic resistance R_{ohmic} and electrode area polarization resistance R_p decrease with increasing operating temperature as shown in Fig. 5.

3.2.3. Arrhenius plots ($R_p \sim 1000/T$) analysis

The Arrhenius plots are determined from impedance spectra and results are shown in Fig. 6. Slopes of the three are similar to each other. It is found that the R_p of electrodes sintered at 900 °C is relatively lower than the other two cases but the 1000 °C cathode sintering case results in the lowest activation energy E_a of 1.28 eV, which is higher than the data by Lu et al. [33] ($E_a = 0.66$ eV of Sm$_{0.5}$Sr$_{0.5}$FeO$_{3-\delta}$–BaZr$_{0.1}$Ce$_{0.7}$Y$_{0.2}$O$_{3-\delta}$ composite cathode for H-SOFC with BZCY electrolyte). The result is better than other SOFCs using BBSM–SDC or BSM or LSM as electrodes as their reported Ea values are in the range of 1.5 eV–2.21 eV [34] for H-SOFCs. Therefore, electrode sintering temperature has certain effect on the activation energy. In practice, the sintering temperature of SFMO–BZCY composite electrode should not exceed 1000 °C, since the 1100 °C case has the worst performance with higher R_p and activation energy.
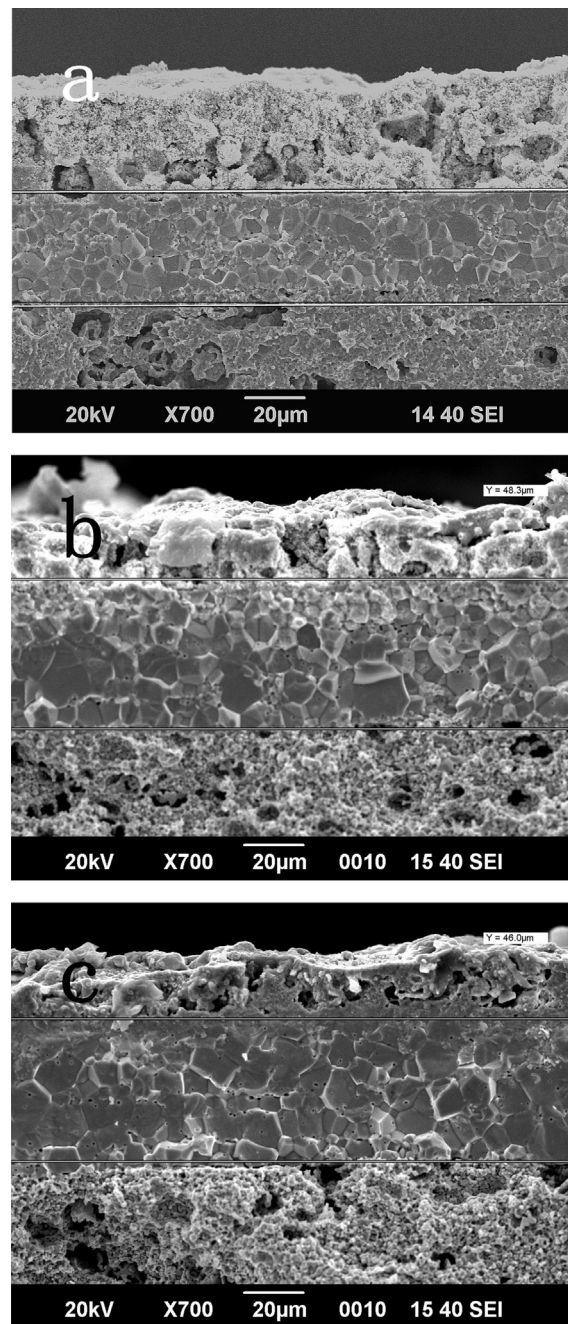

Fig. 7. Cross-sectional views (SEM images) and the microstructures of the interfaces of SFM–BZCY composite cathode, BZCY electrolyte and Ni–BZCY composite anode with different cathode firing temperatures at (a) 900 °C, (b) 1000 °C, and (c) 1100 °C, after electrochemical single fuel cell tests.

3.3. Single fuel cells performance

3.3.1. Microstructure characterization

SEM images of anode supported NiO–BZCY|BZCY|SFM–BZCY cross-session after electrochemical tests are as shown in Fig. 7. Good contacts between the BZCY electrolyte and SFM–BZCY composite cathode layer as well as NiO–BZCY anode are maintained, and no obvious cracks or big pores are found. As shown in Fig. 7, the electrolyte thickness values of three samples are close to each other and are 42 μm, 49 μm, and 45 μm, respectively, which suggests that similar dense and uniform electrolytes can be obtained for different
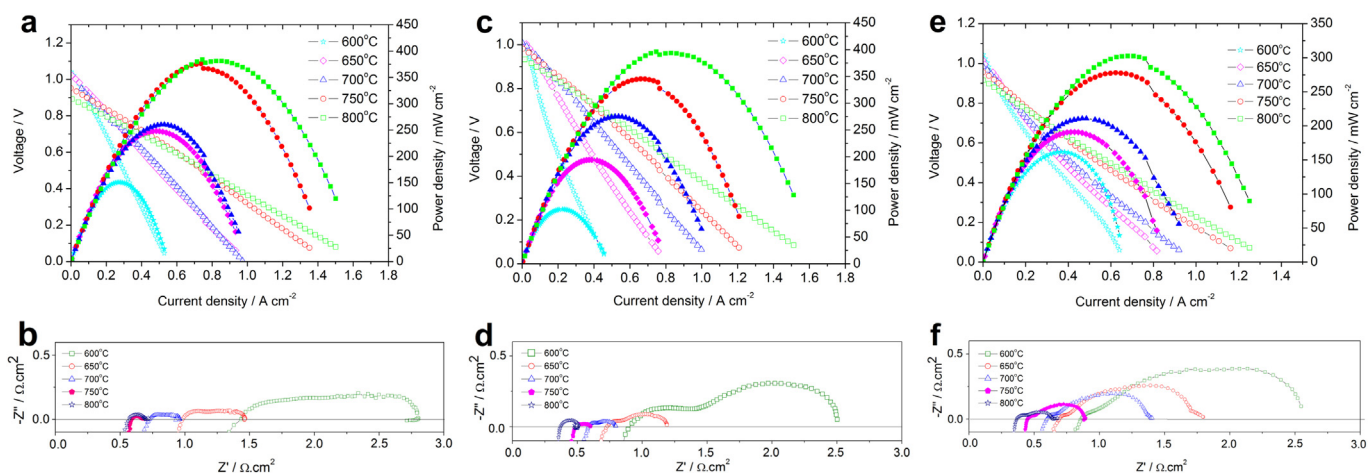
Fig. 8. (a)(c)(e) *I–V* and *I–P* curves measured at test temperature in range of 600 °C–800 °C by a step of 50 °C for the single cells using SFM–BZCY (40:60 weight%) as composite cathodes at co-sintering temperatures of 900 °C, 1000 °C, and 1100 °C, respectively; (b)(d)(f) Impedance spectra figures of symmetrical fuel cells (SFM–BZCY as both electrodes with BZCY as electrolyte material) with cathode sintering temperature at 900 °C, 1000 °C, and 1100 °C, respectively.

sintering temperature cases in this study. Furthermore, cross-sectional SEM results show that high temperature firing causes a certain degree of porosity loss. The thickness of composite cathode is about 20–30 μm while the anode is above 450 μm.

3.3.2. Single fuel cells − sintering temperature analysis

The sintering temperature is purposely varied to evaluate its effect on single cell performance. Tests are conducted for single cells consisting of SFM–BZCY cathode, BZCY electrolyte and NiO–BZCY anode. Fig. 8 shows the current density−voltage (*I–V*) curves and current density−power density (*I–P*) curves of these single cells at operating temperatures from 600 °C to 800 °C. As can be seen from Fig. 8a, c and e, the peak power density (PPD) of single fuel cells increases with increasing operating temperature, although the PPD increment is small from 750 °C to 800 °C. Repeated experiments are conducted but the increment in PPD from 750 °C to 800 °C is still not very large. The reason can be complicated and is not fully understood at the present time. Further detailed study is needed to analyze the microstructure of the electrodes, the ionic conductivity of the electrolyte and the electrochemical reaction mechanisms. The highest power densities at operation temperature of 800 °C are achieved as 383 mW cm^{-2}, 396 mW cm^{-2}, and 302.6 mW cm^{-2} at cathode co-sintering temperature of 900 °C, 1000 °C, and 1100 °C, respectively. These results are much better than even typical O-SOFC with perovskites La$_{0.5}$Sr$_{0.5}$Co$_{0.5}$Ti$_{0.5}$O$_{3-\delta}$ as electrode and La$_{0.8}$Sr$_{0.2}$Ga$_{0.83}$Mn$_{0.17}$O$_{3-\delta}$ as electrolyte achieving best power density as 220 mW cm^{-2} at 800 °C [5]. Compared with other two different cathode sintering conditions, cells with cathode sintering temperature set at 1000 °C is beneficial to achieve higher power density with the open-circuit voltage (OCV) close to 1.0 V. The interfacial area polarization resistances R_p of single fuel cells are measured under the operating temperature range of 600 °C–800 °C and shown in Fig. 8b, d and f. It is clearly observed that single cell fired at 900 °C had the best electrochemical performance with the lowest R_p of 0.101 Ω cm^2 and OCV of about 1.0 V at 800 °C operating condition, which is better than or similar with other H-SOFCs also using BZCY as electrolyte (0.46 Ω cm^2 at 600 °C of Ba$_{0.5}$Sr$_{0.5}$Co$_{0.8}$Fe$_{0.2}$O$_{3-\delta}$–BZCY|BZCY|NiO–BZCY [35]; 0.10 Ω cm^2 at 700 °C of BaCo$_{0.7}$Fe$_{0.2}$Nb$_{0.1}$O$_{3-\delta}$|BZCY|NiO–BZCY [12]; and 0.28 Ω cm^2 at 700 °C of BaCe$_{0.5}$Bi$_{0.5}$Nb$_{0.1}$O$_3$ cathode H-SOFC with BZCY as electrolyte [18]). The values of R_p for H-SOFCs with SFM–BZCY cathode are found to be mainly between 0.1 and 0.5 Ω cm^2 at intermediate temperature (Fig. 8). It should be

mentioned that even the worst R_p of 1.35 Ω cm^2 at 600 °C is better than Pr$_2$NiO$_{4+\delta}$ cathode on BZCY electrolyte of 2.76 Ω cm^2 at the same t_{op} [36]. The lowest R_{ohmic} of these single fuel cells achieves 0.57 Ω cm^2 at 700 °C with cathode being fired at 900 °C. The R_{ohmic} is 0.37 Ω cm^2 at 800 °C with cathode being fired at 1000 °C and 0.142 Ω cm^2 at 700 °C with cathode being fired at 1100 °C. These results clearly demonstrate the potential of SFM–BZCY as a promising cathode for H-SOFC. Lu et al. [33] have reported their maximum power density of 341 mW cm^{-2} and low interfacial polarization resistance of 0.1 Ω cm^2 at 700 °C obtained with BZCY electrolyte and Sm$_{0.5}$Sr$_{0.5}$FeO$_{3-\delta}$–BZCY as composite cathode in a H-SOFC, which are close to our results (341 mW cm^{-2} and 0.19 Ω cm^2) at the same operating temperature. Wu et al. [20] obtained a R_p of 0.21 Ω cm^2 at 700 °C for Sm$_{0.5}$Sr$_{0.5}$CoO$_{3-\delta}$–BaCe$_{0.8}$Sm$_{0.2}$O$_{3-\delta}$ composite cathodes of H-SOFC, which is also close to the present study. Lin et al. [13,37]applied GdBaCo$_2$O$_{5+\delta}$ and SmBaCo$_2$O$_{5+\delta}$ to BZCY electrolyte and obtained lowest R_p of 0.16 Ω cm^2 and 0.15 Ω cm^2 at 700 °C. In another study, Zhao et al. [38] obtained a R_p of 0.15 Ω cm^2 at 700 °C with PrBaCo$_2$O$_{5+\delta}$ cathode (with BZCY electrolyte). The values of R_p obtained in the present study are close to those for other potential cathode materials, indicating that the SFM–BZCY is also promising for use as H-SOFC cathode. However, the best performances of SFM–BZCY|BZCY|NiO–BZCY (lowest R_p of 0.10 Ω cm^2 and peak power density of 396 mW cm^{-2}) are a little lower than those of LSF–SDC (0.074 Ω cm^2 and 543 mW cm^{-2}) [10]. As a comparison, the performances of H-SOFC with different cathode materials are summarized in Table 1. It is clearly demonstrates that the SFM–BZCY is a promising candidate for H-SOFC.

Based on Figs. 2 and 7, cathode at high firing temperature (1100 °C) has relatively large grain size in same cathode thickness scale and relatively denser electrolyte. And electrodes fired at relatively low firing temperature (900 °C) might cause poor adherence between electrolyte and composite cathode, and consequently, bad bonding at the interface, leading to a higher charge transfer resistance and poor fuel cell performance. Thus, the relatively low performance of NiO–BZCY|BZCY|SFM–BZCY single fuel cells here may be caused by relative thicker electrolyte thickness (from Fig. 7, electrolyte thickness is about 50 μm), since reducing the electrolyte thickness to 20 μm can dramatically improve the cell performance [39]. The results on single cell with SFM–BZCY composite cathode demonstrate that 1000 °C cathode sintering temperature offers a relatively better structure for

H-SOFCs with SFM–BZCY cathode, BZCY electrolyte and NiO–BZCY anode.

4. Conclusions

A combination $Sr_2Fe_{1.5}Mo_{0.5}O_6$–$BaZr_{0.1}Ce_{0.7}Y_{0.2}O_{3-\delta}$ (SFM–BZCY) is developed as a composite cathode material for proton-conducting solid oxide fuel cells (H-SOFCs) with BZCY electrolyte. The single cells with the configuration NiO–BZCY|BZCY|SFM–BZCY are manufactured and tested at 600–800 °C in air and wet H_2 (3% H_2O). While the symmetrical fuel cells with the structure of SFM–BZCY|BZCY|SFM–BZCY are also tested under the same intermediate temperature range. All the single fuel cells and symmetrical fuel cells are sintered under three different situations (900 °C, 1000 °C and 1100 °C). The Maximum peak power densities (PPD) of single fuel cells are 383 (sintered at 900 °C), 396 (sintered at 1000 °C) and 303 mW cm^{-2} (sintered at 1100 °C) at 800 °C, respectively, and the interfacial area polarization resistance R_p, typically from 0.101 $\Omega \cdot cm^2$ to 1.67 $\Omega \cdot cm^2$ for all situations. The area R_p of a symmetrical fuel cell achieves its lowest values of 0.088 (sintered at 900 °C), 0.1234 (sintered at 1000 °C) and 0.1849 Ω cm^2 (sintered at 1100 °C) at 800 °C, respectively. Arrhenius plots suggest that the performance of H-SOFCs with BZCY as electrolyte and SFM–BZCY as composite cathode under the sintering temperature of 1000 °C is much better than others. The present study demonstrates that the SFM–BZCY composite cathode is a promising material for H-SOFC cathode.

Acknowledgments

References

[1] A.J. Jacobson, Chem. Mater. 22 (2010) 660–674.
[2] B. Zhu, Int. J. Energy Res. 33 (2009) 1126–1137.
[3] N.Q. Minh, Solid State Ionics 174 (2004) 271–277.
[4] X.J. Liu, D. Han, Y.C. Zhou, X. Meng, H. Wu, J.L. Li, F.R. Zeng, J. Power Sources 246 (2014) 457–463.
[5] R.M. Coronado, A. Aguadero, D.P. Coll, L. Troncoso, J.A. Alonso, M.T.F. Díaz, Int. J. Hydrogen Energy 37 (2012) 18310–18318.
[6] J.C. Vázquez, J.C.R. Morales, D. Marrero-López, J.P. Martínez, P. Núñez, Pedro Gómez-Romero, J. Power Sources 171 (2007) 552–557.
[7] D.M. Bastidas, S. Tao, J.T.S. Irvine, J. Mater. Chem. 16 (2006) 1603–1605.
[8] Y.H. Huang, R.I. Dass, Z.L. Xing, J.B. Goodenough, Chem. Inf. 312 (2006) 254–257.
[9] M.F. Liu, J.F. Gao, X.Q. Liu, G.Y. Meng, Int. J. Hydrogen Energy 36 (2011) 13741–13745.
[10] W.P. Sun, Z.W. Zhu, Y.X. Jiang, Z. Shi, L.T. Yan, W. Liu, Int. J. Hydrogen Energy 36 (2011) 9956–9966.
[11] W.P. Sun, L.T. Yan, B. Lin, S.Q. Zhang, W. Liu, J. Power Sources 195 (2010) 3155–3158.
[12] Y. Lin, W. Zhou, J. Sunarso, R. Ran, Z.P. Shao, Int. J. Hydrogen Energy 37 (2012) 484–497.
[13] B. Lin, S.Q. Zhang, L.C. Zhang, L. Bi, H.P. Ding, X.Q. Liu, J.F. Gao, G.Y. Meng, J. Power Sources 177 (2008) 330–333.
[14] Z. Ling, C.R. Xia, Eng. Sci. 2 (2013) 88–97.
[15] H. Yamaura, T. Ikuta, H. Yahiro, G. Okada, Solid State Ionics 176 (2005) 269–274.
[16] Y. Lin, R. Ran, Y. Zheng, Z.P. Shao, W.Q. Jin, N.P. Xu, J. Ahn, J. Power Sources 180 (2008) 15–22.
[17] Y.H. Ling, J. Yu, B. Lin, X.Z. Zhang, L. Zhao, X.Q. Liu, J. Power Sources 196 (2011) 2631–2634.
[18] Z.T. Tao, L. Bi, L.T. Yan, W.P. Sun, Z.W. Zhu, R.R. Peng, W. Liu, Electrochem. Commun. 11 (2009) 688–690.
[20] T.Z. Wu, R.R. Peng, C.R. Xia, Solid State Ionics 179 (2008) l505–1508.
[21] M. Kumar, S. Srikanth, B. Ravikumar, T.C. Alex, S.K. Das, Mater. Chem. Phys. 113 (2009) 803–815.
[22] J. Linden, T. Yamamoto, M. Karppinen, H. Yamauchi, T. Pietari, J. Appl. Phys. Lett. 76 (2000) 2925–2927.
[23] Z.M. Wang, Y. Tian, Y.D. Li, J. Power Sources 196 (2011) 6104–6109.
[24] N.N. Dai, Z.H. Wang, Z.L. Lou, Y.M. Yan, J.S. Qiao, J. Peng, K.N. Sun, J. Power Sources 217 (2012) 519–523.
[25] N.N. Dai, Z.L. Lou, Z.H. Wang, X.X. Liu, Y.M. Yan, J.S. Qiao, T.Z. Jiang, K.N. Sun, J. Power Sources 243 (2013) 766–772.
[26] L. Zhang, Y.Q. Liu, Y.X. Zhang, G.L. Xiao, F.L. Chen, C.R. Xia, Electrochem. Commun. 13 (2011) 711–713.
[27] J.H. Wright, A.V. Virkar, Q. Liu, F.L. Chen, J. Power Sources 237 (2013) 13–18.
[28] Q. Liu, D.E. Bugaris, G.L. Xiao, M. Chmara, S.G. Ma, H.C. z-Loye, M.D. Amiridis, F.L. Chen, J. Power Sources 196 (2011) 9148–9153.
[29] P. Sawant, S. Varma, B.N. Wani, S.R. Bharadwaj, Int. J. Hydrogen Energy 37 (2012) 3848–3856.
[30] Q.M. Jiang, Master Degree Thesis, 2012.
[31] B.B. He, L. Zhao, S.X. Song, T. Liu, F.L. Chen, C.R. Xia, J. Electrochem. Soc. 159 (2012) 13619–13626.
[32] Q. Liu, C.H. Yang, X.H. Dong, F.L. Chen, Int. J. Hydrogen Energy 35 (2010) 10039–10044.
[33] X.Y. Lu, Y.H. Chen, Y.Z. Ding, B. Lin, Int. J. Hydrogen Energy 37 (2012) 8630–8634.
[34] B.B. Liu, Z.Y. Jiang, B. Ding, F.L. Chen, C.R. Xia, J. Power Sources 196 (2011) 999–1005.
[35] Y. Yoo, N. Lim, J. Power Sources 229 (2013) 48–57.
[36] D. Pergolesi, E. Fabbri, A. D'Epifanio, E. Di Bartolomeo, A. Tebano, S. Sanna, et al., Nat. Mater. 9 (2010) 846–852.
[37] B. Lin, Y.C. Dong, R.Q. Yan, S.Q. Zhang, M.J. Hu, G.Y. Meng, J. Power Sources 186 (2009) 446–449.
[38] L. Zhao, B.B. He, B. Lin, R.R. Peng, G.Y. Meng, X.Q. Liu, J. Power Sources 194 (2009) 835–837.
[39] T.Z. Wu, R.R. Peng, C.R. Xia, Solid State Ionics 179 (2008) 1505–1508.